ceramics

MDPI

Article

Hafnium-Zirconium Carbonitride (Hf,Zr)(C,N) by One Step Mechanically Induced Self-Sustaining Reaction: Powder Synthesis and Spark Plasma Sintering

Irina Khadyrova [1], Veronika Suvorova [1,*], Andrey Nepapushev [1], Dmitrii Suvorov [2], Kirill Kuskov [1,2] and Dmitry Moskovskikh [1]

[1] Center of Functional Nano-Ceramics, National University of Science and Technology MISIS, Leninskiy Prospekt, 4, 119049 Moscow, Russia; irina.khadyrova@mail.ru (I.K.); anepapushev@gmail.com (A.N.); kkuskov@misis.ru (K.K.); mos@misis.ru (D.M.)

[2] Department of Functional Nanosystems and High Temperature Materials, National University of Science and Technology MISIS, Leninskiy Prospekt, 4, 119049 Moscow, Russia; suvorov.ds@misis.ru

* Correspondence: buynevich.vs@misis.ru

Abstract: Nanostructured single-phase hafnium-zirconium carbonitride powders were synthesized using a simple and fast mechanochemical synthesis approach. The critical milling duration, after which a (Hf,Zr)(C,N) solid solution formation inside a jar occurred via mechanically induced self-sustained reaction (MSR), was 10 min. After 30 min of treatment, a solid-gas reaction was completed, and as a result, a homogeneous (Hf,Zr)(C,N) powder consisting of 10–500 nm submicron particles was obtained. The phase and structure evolution of the powders after different treatment durations allowed for the establishment of possible reaction mechanisms, which included the formation of Hf/Zr/C-layered composite particles, their interaction via MSR, and further grinding and nitridization. Spark plasma sintering (SPS) was used to produce bulk hafnium-zirconium carbonitride ceramics from nanostructured powder. The sample had higher values of relative density, hardness, and fracture toughness than those for binary compounds of a similar composition.

Keywords: ultra-high-temperature ceramics; hafnium zirconium carbonitride; high energy ball milling; mechanically induced self-sustaining reaction; spark plasma sintering; mechanical properties

Citation: Khadyrova, I.; Suvorova, V.; Nepapushev, A.; Suvorov, D.; Kuskov, K.; Moskovskikh, D. Hafnium-Zirconium Carbonitride (Hf,Zr)(C,N) by One Step Mechanically Induced Self-Sustaining Reaction: Powder Synthesis and Spark Plasma Sintering. *Ceramics* **2023**, *6*, 1129–1138. https://doi.org/10.3390/ceramics6020067

Academic Editors: Margarita A. Goldberg and Elisa Torresani

Received: 20 April 2023
Revised: 10 May 2023
Accepted: 15 May 2023
Published: 17 May 2023

1. Introduction

The development of new materials capable of withstanding high temperatures during aerodynamic heating (>2000 °C) is of particular interest among scientists involved in the research of ultra-high-temperature compounds [1–3]. Borides, carbides, and nitrides of transition metals of groups IV and V, known as ultra-high-temperature ceramics (UHTC), are typically used to create new compounds for use in extreme environments. The presence of strong atomic covalent bonds in these compounds determines their extreme melting temperatures (>3000 °C), high mechanical properties, electrical and thermal conductivity, oxidation resistance, chemical and phase stability, as well as their ability to withstand extreme temperatures [4,5].

From the standpoint of mechanical and thermophysical properties, more complex compounds, such as carbonitrides of transition metals, are advantageous due to the hybridization of electron orbitals upon the substitution of atoms in the metallic and nonmetallic sublattices. The properties of these compounds are dependent on the C/N ratio and surpass the properties of ordinary binary Me-C and Me-N compounds, including those at elevated temperatures [6,7]. For example, Lu Yang et al. [8] studied the effect of the C/N ratio in Ti(C_{1-x},N_x)-based cermet substrates and in TiN/Ti(C,N)/Al_2O_3/TiN coatings on the high-temperature frictional properties of CVD coatings. It was demonstrated that by varying the C/N ratio, it was possible to influence the structure of the substrate and

coatings, increasing their hardness and friction properties. In other words, it is possible to adjust the necessary parameters depending on the required functional characteristics. Harrison et al. reported [9] that the thermophysical properties of ZrC_xN_y ceramic material obtained by carbothermic reduction were superior to those of zirconium carbides and nitrides. Due to the growing contribution of the electronic part to the thermal conductivity, its value increased with the increase of the N content in the ZrC_xN_y, which ranged from 40–50 $W \cdot m^{-1} \cdot K^{-1}$. As well as being used as protective wear-resistant coatings [10,11], carbonite ceramics are also used to improve the mechanical properties and oxidation resistance of carbon–carbon composites [12].

Unlike traditional methods of synthesis [13–15], which require long-duration and energy-consuming treatment, mechanochemical synthesis (MS) is a fast and simple method for obtaining various compounds with the required composition. This process typically involves the mechanical activation of a 'solid-solid' reaction between components of a powder mixture during its treatment in different ball mills. However, the process can be conducted in a reactive gas atmosphere (e.g., N_2, NH_3, H_2), allowing for a 'solid-gas' interaction and the formation of nitrides and hydrates. For example, plasma-assisted ball milling was used to rapidly obtain Mg_3N_2, TiH_2, and TiN powders [16], as well as more complex HfC_xN_y compounds [17]. Alternatively, with the participation of a gaseous reagent, MS can be carried out in a high-energy planetary ball mill, which allows for the shortening of the processing duration to up to 30–90 min [18]. During the high-energy ball milling (HEBM) of reactive compounds, two types of reaction may occur: in the first case, the chemical interaction between the components proceeds gradually over time, leading to the slow formation of a product. In the second case, the HEBM of exothermic powder mixtures leads to the initiation of a fast combustion reaction in a jar—a mechanically induced self-propagating reaction (MSR). With the appropriate synthesis parameters, MSR can be used to obtain single-phase complex compounds of carbonitrides as well as double and more complex carbides [19–21]. One advantage of the MSR synthesis method is the possibility for a precise morphology and structure control of the synthesized powders. This approach was used to synthesize nanocrystalline titanium-niobium carbonitride $Ti_yNb_{1-y}C_xN_{1-x}$ powders with a uniform chemical composition [22].

In this work, hafnium-zirconium carbonitride (Hf,Zr)(C,N) powders were synthesized by MSR via treatment in a high-energy planetary ball mill of elementary hafnium, zirconium, and carbon powders in a nitrogen atmosphere. The evolution of the phase composition and microstructure of the powders was studied as a function of the HEBM duration. The bulk hafnium-zirconium carbonitride was produced by spark plasma sintering (SPS) method, and its physical and mechanical properties were also studied.

2. Materials and Methods

The experiments were carried out with hafnium (purity 98.7%), zirconium (purity 99.9%), and carbon black (purity 99.5%) powders, which were treated in gaseous nitrogen (purity 99.5%). The HEBM of the Hf + Zr + C powder mixture (85.5 wt% Hf, 10.89 wt% Zr, and 3.61 wt% C) was carried out in an "Activator-2S" high-energy planetary ball mill (LLC Activator, Novosibirsk, Russia) in steel jars with steel grinding media. The jar rotation speed was 694 rpm, the rotation coefficient K = 1.0, and the duration t was 5, 9, 10, 15, 20, and 30 min. Nitrogen pressure was 0.6 MPa in the jars, and the ball-to-powder ratio was 20:1.

Bulk (Hf,Zr)(C,N) samples with a diameter of 12.7 ± 1 mm and a thickness of 2–3 mm were obtained by SPS on a Labox 650 setup (SinterLand, Nagaoka, Japan). The sintering was carried out in an argon atmosphere (0.08 MPa) at a heating rate of 100 °C/min to a maximum temperature of 1900 °C with a holding time of 20 min. Throughout the entire SPS process, an external load of 50 MPa was applied.

The microstructure of powder samples was studied using scanning electron microscopy (SEM) on a JEOL JSM7600F (JEOL Ltd., Tokio, Japan) device equipped with an X-MAX 80 mm^2 (Oxford Instruments, Abingdon, UK) detector for energy-dispersive

X-ray spectroscopy (EDS) and AZtec software (Oxford Instruments, Abingdon, UK) to build element distribution maps and composition profiles. The shooting was carried out in the secondary electrons SE and backscattering BSE regimes at an accelerating voltage of 15 kV.

The phase composition of the powders after different HEBM durations as well as of the consolidated samples was studied by X-ray phase analysis (XRD) on a Difrey-401 diffractometer (JSC Scientific Instruments, Saint Petersburg, Russia). The samples were analyzed using the Bragg–Brentano focusing geometry without monochromatization of the incident and reflected radiation. The X-ray diffraction patterns were recorded using the Cr-Kα wavelength (λ = 0.22909 nm). The analysis was carried out in the 2θ range from 30° to 140°, and the patterns were recorded with a step $\Delta 2\theta$ = 0.1° and a signal accumulation time t = 2 s. The identification of the phases present in the samples was carried out based on the ICDD PDF-4 database using the Match-3 and Maud software package version 2.94 [23].

The pycnometric density (ρ_p) of the consolidated samples was measured by gas pycnometry using an AccuPyc 1340 setup (Micromeritics, Norcross, GA, USA). The hydrostatic density (ρ_h) of the samples was determined by hydrostatic weighing. The corresponding masses were obtained by weighing the samples on an analytical balance in air and in distilled water (ρ_w = 0.9978 g/cm^3) after applying a thin layer of Vaseline to the surface to cover open porosity (ρ_l = 0.870 g/cm^3). The relative density of the samples after SPS ρ (%) was determined as the ratio of hydrostatic density (ρ_h) to pycnometric density (ρ_p).

The microhardness (HV) and fracture toughness (K_1C) of sintered samples were measured by the Vickers method using a Durascan 70 digital hardness tester (Struers ApS, Ballerup, Denmark) with a diamond indenter in the form of a tetrahedral pyramid with an apex angle of 136°. The maximum load was 30 N, and the exposure time was 20 s. When the load was removed, the diagonals of the imprint remaining on the surface of the sample were measured along with the length of the cracks.

To determine the Young's modulus, the sintered sample was indented under an applied load of 100 mN and an exposure time of 10 s on a Micro-Hardness Tester (CSM Instruments, Peseux, Switzerland). After measurements, the numerical value of the Young's modulus was determined by the slope of the unloading curve. The fracture resistance is calculated using the Anstis formula [24].

3. Results and Discussion

A high-energy mechanical treatment of a hafnium, zirconium, and carbon powder mixture was carried out for 5–30 min in a nitrogen atmosphere. Figure 1 shows the diffraction patterns of the initial mixture and the powders after different HEBM durations. Based on the XRD results, the powder mixture consisted of individual Hf and Zr after 5 min of HEBM.

After 9 min of HEBM, low-intensity peaks of a NaCl-type solid solution were detected on the diffraction pattern, which indicated the beginning of a chemical interaction between the components of the mixture and the formation of a new-phase nucleus. The phase composition changed drastically after 10 min of HEBM due to the mechanically induced reaction. The powder consisted predominantly of hafnium-zirconium carbonitride (Hf,Zr)(C,N), while some Hf and Zr remained unreacted after the reaction. After 20 min of HEBM, individual peaks of hafnium and zirconium were still present in the diffraction pattern, and only an increase in the mechanical treatment duration to 30 min allowed for a complete reaction and the formation of a single-phase (Hf,Zr)(C,N) carbonitride.

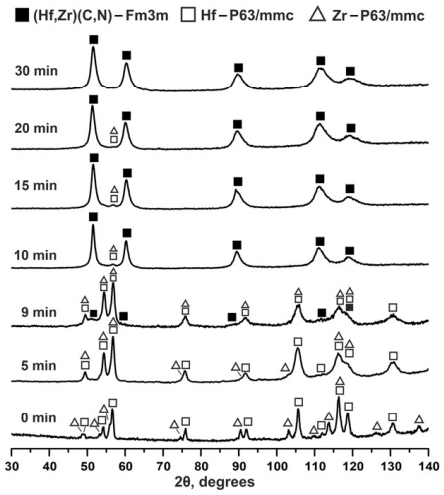

Figure 1. *X*-ray diffraction patterns of the initial Hf + Zr + C powder mixture and after HEBM in a nitrogen atmosphere, depending on the different treatment durations.

The dependence of the (Hf,Zr)(C,N) lattice parameter a (nm) on the HEBM duration was studied (Table 1). The lattice parameter decreased over the entire treatment interval from 10 to 30 min, indicating that nitrogen atoms were introduced into the (Hf,Zr)(C,N) lattice and that the nitridation degree increased with the increase of the HEBM duration.

Table 1. The interplanar distances and lattice parameters of reference binary compounds and hafnium-zirconium carbonitride after different HEBM durations.

Sample	HEBM Duration, min	(111)	(200)	(220)	(311)	(222)	a, nm
HfC (#39-1491)	-	2.6776	2.3189	1.6401	1.3983	1.3389	0.4638
ZrC (#35-0784)	-	2.7089	2.3459	1.6592	1.4149	1.3547	0.4693
HfN (#33-0592)	-	2.6120	2.2620	1.6002	1.3641	1.3061	0.4525
ZrN (#02-0956)	-	2.64	2.29	1.62	1.38	1.32	0.456
(Hf,Zr)(C,N)	10	2.6342	2.2817	1.6273	1.3889	1.3296	0.4588
	15	2.6332	2.2803	1.6268	1.3871	1.3289	0.4585
	20	2.6330	2.2801	1.6245	1.3863	1.3283	0.4583
	30	2.6328	2.2792	1.6225	1.3838	1.3268	0.4578

The microstructures of the samples and the distribution of elements after different HEBM durations are shown in Figure 2. The initial Hf + Zr + C mixture (Figure 2a) consisted of individual particles of hafnium, zirconium, and carbon black with different morphologies. Carbon black was found in the form of agglomerates of up to 200 μm, and hafnium and zirconium particles were in the range of 20 to 250 μm. The short-term mechanical treatment (Figure 2b) contributed to the grinding of the initial components of the mixture, their flattening, and the cleaning of the surfaces from the oxide films. Through HEBM, atomically clean planes were formed, through which the flattened particles welded to each other, creating layered Hf/Zr/C composite particles. With an increase in the HEBM duration to 9 min (Figure 2c), the tendency for grinding remained, and the thickness of the layers in the Hf/Zr/C composite particles decreased to 0.2–2 μm. It is clear from the structure of the powder that the mechanically induced self-sustained reaction occurred between 9 and 10 min of HEBM. Figure 2d shows that the powder consisted mainly of agglomerates of submicron rounded particles after 10 min, which indicated the occurrence of a combustion reaction and crystallization from the melt [25,26].

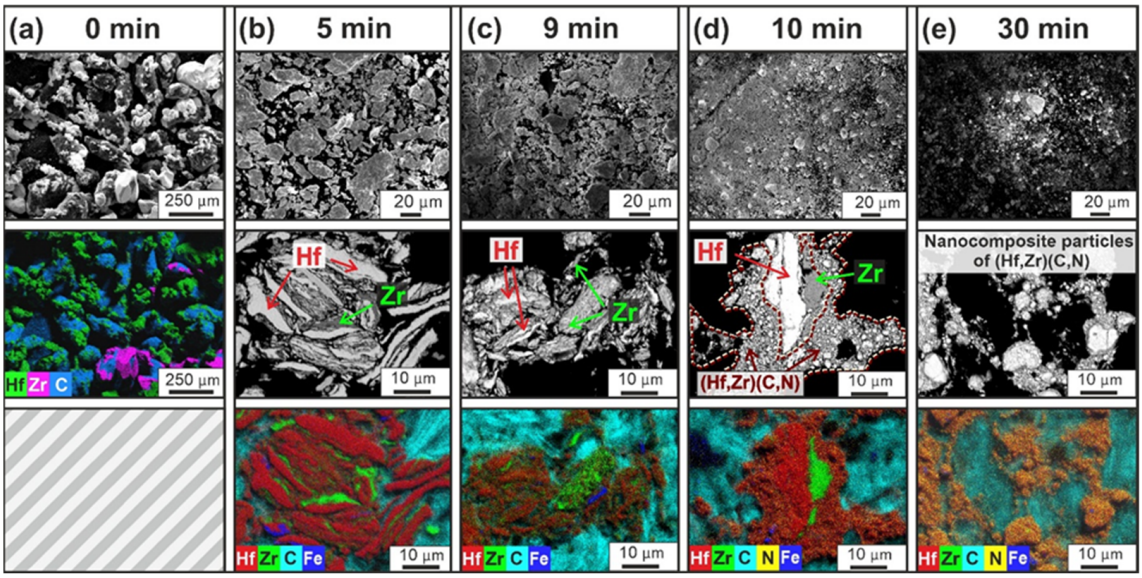

Figure 2. SEM images and distribution of elements for the Hf + Zr + C powder mixtures after (**a**) 0, (**b**) 5, (**c**) 9, (**d**) 10, and (**e**) 30 min of HEBM in a nitrogen atmosphere.

Apparently, repeated processes of destruction and cold welding [27] during HEBM led to the accumulation of defects as well as to a decrease in the diffusion distance between Hf, Zr, and C in Hf/Zr/C composite particles and, consequently, to a decrease in the activation energy and increase in the reactivity of the mixture. Intense local heating due to friction forces, accumulated defects, and high exothermicity of the powder mixture [28,29] contributed to the initiation of a self-propagating reaction inside the jars, as a result of which the (Hf,Zr)(C,N) product was formed instantly. However, it should be noted that after 10 min, the reaction was incomplete. There were still agglomerates with a layered structure in the powder, which consisted mainly of submicron particles. A solid solution was found along the edges of the particles, and hafnium and zirconium layers about 5 μm thick were found in the central part of a submicron particle (Figure 2d). With an increase in the duration of the HEBM, the grinding of unreacted metals and solid-solution particles was promoted, resulting in the creation of new active surfaces capable of forming (Hf,Zr)(C,N) (Figure 2e). According to the EDS analysis, the synthesis product (Figure 2b–e) contained iron inclusions, which can be explained by the interaction of the mixture with the material of the steel jars and balls. After 30 min, the powder consisted of agglomerates (Figure 3a) of submicron (Hf,Zr)(C,N) particles ranging in size 10–500 nm (Figure 3b).

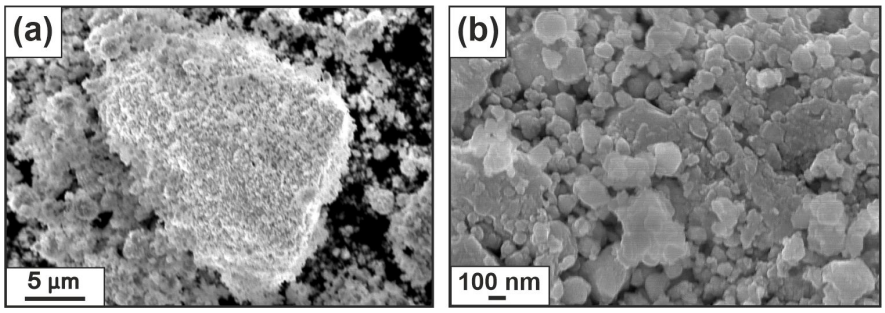

Figure 3. SEM images of (Hf,Zr)(C,N) powder after 30 min of HEBM at different magnifications of (**a**) ×3500 and (**b**) ×50,000.

The EDS results showed that the nitrogen N atomic content was dependent on the HEBM duration (min) (Figure 4). After 5 min of HEBM, no nitrogen was found in the composite particles. During the interval between 5 and 15 min of HEBM, the amount of

nitrogen in the system began to gradually increase from 0 to 4 at%. With a further increase in the treatment duration from 15 to 30 min, the nitrogen content continued to grow, which was in good agreement with the XRD results (Table 1). After 30 min of HEBM, the nitrogen content in the powder was ~12 at%.

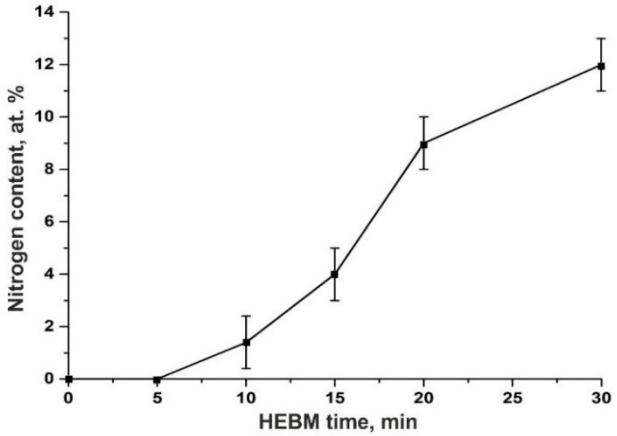

Figure 4. Dependence of the nitrogen content on the HEBM duration.

Considering the XRD and SEM results, it can be concluded that during the HEBM process of a Hf + Zr + C powder mixture in a nitrogen atmosphere, the formation of a solid solution proceeded according to several stages (Figure 5). In the first stage, due to the grinding and plastic deformation of the precursor powders (Figure 5a), layered Hf/Zr/C composite particles were formed, in which the diffusion distances between Hf, Zr, and C were decreased (Figure 5b). At the second stage (Figure 5c), intense local heating led to the occurrence of a mechanically induced self-sustaining reaction. As a result, (Hf,Zr)(C,N) particles with a low nitridation degree (~1 at% N) and partially unreacted hafnium and zirconium were formed. The final stage (Figure 5d) was characterized by the formation of fully reacted submicron (Hf,Zr)(C,N) particles ranging in size 10–500 nm.

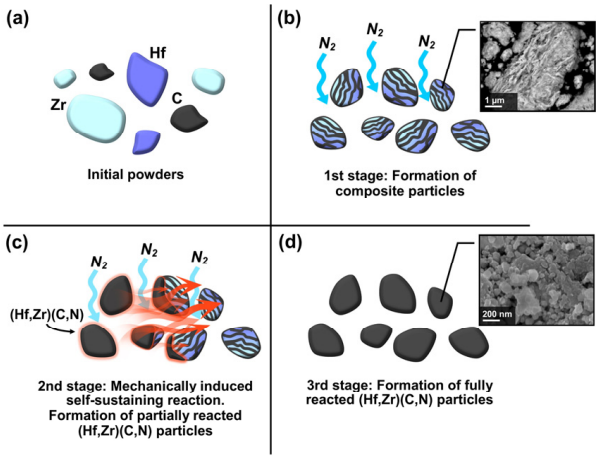

Figure 5. Possible formation mechanism of the (Hf,Zr)(C,N) solid solution during HEBM process: (**a**) initial powders, (**b**) 1st stage: formation of composite particles, (**c**) 2nd stage: mechanically induced self-sustaining reaction, formation of partially reacted (Hf,Zr)(C,N) particles, (**d**) 3rd stage: formation of fully reacted (Hf,Zr)(C,N) particles.

The synthesized submicron hafnium-zirconium carbonitride powder was consolidated by SPS at a temperature of 1900 °C, a constant pressure of 50 MPa, and a holding time of 20 min. The diffraction patterns of the MS product (30 min) and consolidated sample are shown in Figure 6. After SPS, the hafnium-zirconium carbonitride peaks became more

narrow and more intense due to the ordering of the crystal structure and an increase in the crystallites' size after sintering. The peaks of the tetragonal zirconium oxide ZrO_2 (P42/nmc) were also observed after consolidation. After SPS, the lattice parameter for the (Hf,Zr)(C,N) compound was 0.4578 nm.

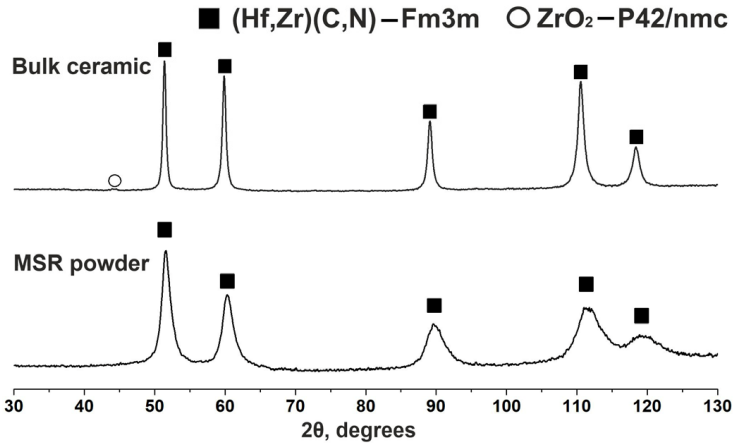

Figure 6. *X*-ray diffraction patterns of the mechanically synthesized (Hf,Zr)(C,N) powder and corresponding bulk ceramics.

Figure 7 illustrates the microstructure of the sintered sample and the distribution of the elements. The bulk material consists of (Hf,Zr)(C,N) grains (gray areas, Figure 7b) ranging in size 3–15 µm (Figure 7a). The dark areas on the micrograph correspond to ZrO_2 (Figure 7b). The oxygen content did not exceed 2 wt%.

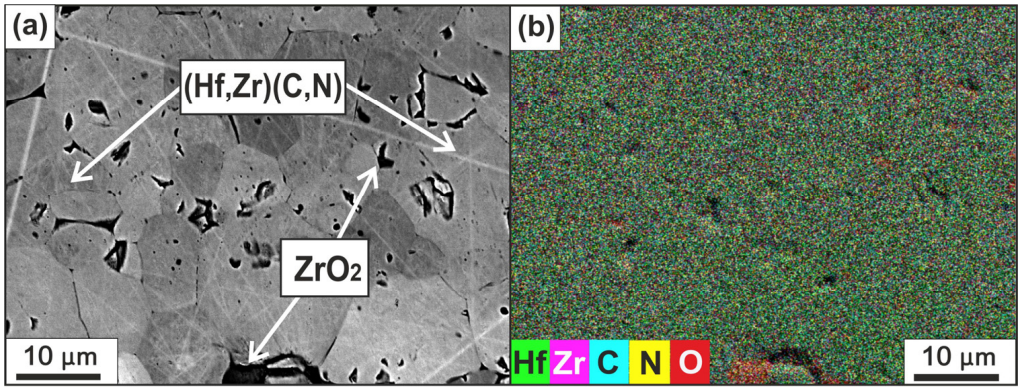

Figure 7. (**a**) Microstructure and (**b**) elemental map distribution of the consolidated (Hf,Zr)(C,N) ceramics.

Table 2 presents the densities measured by hydrostatic weighing (ρ_h) and helium pycnometry (ρ_p), as well as the calculated relative density, which was 97 ± 1%. In addition, Table 2 shows the mechanical properties of bulk hafnium-zirconium carbonitride, as well as that of more complex compounds. The hardness, fracture toughness, and Young's modulus of the obtained (Hf,Zr)(C,N) are comparable to those of binary and multicomponent carbides and carbonitrides.

Table 2. Mechanical properties of consolidated (Hf,Zr)(C,N) ceramics in comparison with other ceramic materials.

Sample	ρ_h, g/cm^3	ρ_p, g/cm^3	ρ, %	HV, GPa	Fracture Toughness K_{1C}, MPa·m$^{1/2}$	Young's Modulus, GPa
(Hf,Zr)(C,N)	10.9	11.3	97 ± 1	17.3 ± 0.5 (30 N)	4.5 ± 0.4	450 ± 20
ZrC [30]	–	–	98.2	16.4 ± 1.3	3.1 ± 0.7	210 ± 19
$HfZrC_2$ [31]	–	–	–	19 ± 1.6 (100 mN)	3.82	466 ± 81
$HfC_{0.5}N_{0.2}$ [32]	–	–	95.6 ± 1	20.8 ± 1 (10 N)	3.5 ± 0.2	~460
(Ta,Hf)CN [33]	–	–	98 ± 1	19.4 ± 0.2 (30 N)	5.4 ± 0.4	591
(Ti,V,Nb,Ta,Mo)(C,N) [34]	–	–	99.8	24.0 ± 0.7 (9.8 N)	4.87 ± 0.25	–
(Zr,Ti)(C,N)–SiC [35]	–	–	98.5 ± 1	17.7–22.4 (9.8 N)	3.0–4.4	–
(Ti,W)(C,N) [36]	–	–	–	15.9–17.8 (30 N)	4.0–4.57	429–481

4. Conclusions

Single-phase hafnium-zirconium carbonitride powders were mechanochemically synthesized in a planetary ball mill by treating elemental Hf, Zr, and C powders in a nitrogen atmosphere. A study of the phase evolution and structure formation, as well as the nitridization kinetics during HEBM, allowed us to establish the formation mechanism of hafnium-zirconium carbonitride powder. It was possible to obtain a solid solution of (Hf,Zr)(C,N) after short-term (10 min) HEBM due to a mechanically induced self-sustaining reaction occurring in the jars. An increase in the HEBM duration promoted further grinding of the powder media and stimulated the formation of new active surfaces that were able to interact with gaseous nitrogen. Following the above-mentioned processes, a single-phase powder with a characteristic grain size in the range of 10–500 nm was formed after 30 min of HEBM.

The consolidation of the (Hf,Zr)(C,N) samples by SPS at a temperature of 1900 °C, an external load of 50 MPa, and a holding time of 20 min led to the production of bulk high-density ceramic material. Carbonitride exhibited a relative density of 97% with a high hardness of 17 ± 0.2 GPa and fracture toughness of 4.5 ± 0.4 MPa·m$^{1/2}$. The mechanical properties of the (Hf,Zr)(C,N) ceramics were comparable to or even higher than those of binary precursor compounds and double carbides.

Author Contributions: Conceptualization, I.K., V.S. and A.N.; methodology, I.K., V.S., A.N., D.S., K.K. and D.M.; investigation, I.K., V.S., A.N., D.S., K.K. and D.M.; resources, D.M.; data curation, V.S.; writing—original draft preparation, V.S. and I.K.; writing—review and editing, V.S., A.N. and K.K.; visualization, V.S.; supervision, A.N.; project administration, A.N. and D.M.; funding acquisition, D.M. All authors have read and agreed to the published version of the manuscript.

Funding: This work was funded by the Russian Science Foundation grant no. 19-79-10280.

Institutional Review Board Statement: Not applicable.

Informed Consent Statement: Not applicable.

Data Availability Statement: Not applicable.

Conflicts of Interest: The authors declare no conflict of interest.

References

1. Talmy, I.G.; Zaykoski, J.A.; Opeka, M.M. High-Temperature Chemistry and Oxidation of ZrB_2Ceramics Containing SiC, Si_3N_4, Ta_5Si_3, and $TaSi_2$. *J. Am. Ceram. Soc.* **2008**, *91*, 2250–2257. [CrossRef]
2. Sciti, D.; Medri, V.; Silvestroni, L. Oxidation behaviour of HfB_2–15 vol.% $TaSi_2$ at low, intermediate and high temperatures. *Scr. Mater.* **2010**, *63*, 601–604. [CrossRef]
3. Balaceanu, M.; Petreus, T.; Braic, V.; Zoita, C.N.; Vladescu, A.; Cotrutz, C.E.; Braic, M. Characterization of Zr-based hard coatings for medical implant applications. *Surf. Coat. Technol.* **2010**, *204*, 2046–2050. [CrossRef]
4. Fahrenholtz, W.G.; Hilmas, G.E.; Talmy, I.G.; Zaykoski, J.A. Refractory Diborides of Zirconium and Hafnium. *J. Am. Ceram. Soc.* **2007**, *90*, 1347–1364. [CrossRef]
5. Marschall, J.; Pejaković, D.A.; Fahrenholtz, W.G.; Hilmas, G.E.; Zhu, S.; Ridge, J.; Fletcher, D.G.; Asma, C.O.; Thoemel, J. Oxidation of ZrB_2-SiC Ultrahigh-Temperature Ceramic Composites in Dissociated Air. *J. Thermophys. Heat Transf.* **2009**, *23*, 267–278. [CrossRef]
6. Kurbatkina, V.V.; Patsera, E.I.; Levashov, E.A.; Vorotilo, S. SHS Processing and Consolidation of Ta–Ti–C, Ta–Zr–C, and Ta–Hf–C Carbides for Ultra-High-Temperatures Application. *Adv. Eng. Mater.* **2018**, *20*, 1701075. [CrossRef]
7. Vogel, F.; Ngai, S.; Smith, C.J.; Holler, R.; Thompson, G.B. Complex evaporation behavior of a transition metal carbo-nitride (Hf(C,N)) studied by atom probe tomography. *Ultramicroscopy* **2018**, *194*, 154–166. [CrossRef]
8. Yang, L.; Xiong, J.; Chen, X.; Li, X.; Deng, C.; Zhang, D.; Yi, L. Study on the growth and wear characters of CVD coating deposited on Ti(C, N)-based cermets with adding different C/N ratios of Ti(C, N) powders. *Ceram. Int.* **2023**, *49*, 18023–18034. [CrossRef]
9. Harrison, R.; Ridd, O.; Jayaseelan, D.D.; Lee, W.E. Thermophysical characterisation of ZrCxNy ceramics fabricated via carbothermic reduction–nitridation. *J. Nucl. Mater.* **2014**, *454*, 46–53. [CrossRef]
10. Liang, L.; Wei, B.; Wang, D.; Fang, W.; Chen, L.; Wang, Y. Densification, microstructures, and mechanical properties of (Zr, Ti)(C, N) ceramics fabricated by spark plasma sintering. *J. Eur. Ceram. Soc.* **2022**, *42*, 6445–6456. [CrossRef]
11. Braic, M.; Balaceanu, M.; Vladescu, A.; Zoita, C.N.; Braic, V. Study of (Zr,Ti)CN, (Zr,Hf)CN and (Zr,Nb)CN films prepared by reactive magnetron sputtering. *Thin Solid. Films* **2011**, *519*, 4092–4096. [CrossRef]
12. Miao, Q.; Fu, Y.; Chen, H.; Zhang, J.; Zhao, J.; Zhang, Y. Simultaneous enhancement of mechanical and ablation properties of C/C composites modified by (Hf-Ta-Zr)C solid solution ceramics. *J. Eur. Ceram. Soc.* **2023**, *43*, 3182–3190. [CrossRef]
13. Wu, K.-H.; Jiang, Y.; Jiao, S.-Q.; Chou, K.-C.; Zhang, G.-H. Preparations of titanium nitride, titanium carbonitride and titanium carbide via a two-step carbothermic reduction method. *J. Solid. State Chem.* **2019**, *277*, 793–803. [CrossRef]
14. Yudin, S.N.; Kasimtsev, A.V.; Volodko, S.S.; Alimov, I.A.; Markova, G.V.; Sviridova, T.A.; Tabachkova, N.Y.; Buinevich, V.S.; Nepapushev, A.A.; Moskovskikh, D.O. Low-temperature synthesis of ultra-high-temperature HfC and HfCN nanoparticles. *Materialia* **2022**, *22*, 101415. [CrossRef]
15. Vasanthakumar, K.; Ghosh, S.; Koundinya, N.T.B.N.; Ramaprabhu, S.; Bakshi, S.R. Synthesis and mechanical properties of TiC_x and Ti(C,N) reinforced Titanium matrix in situ composites by reactive spark plasma sintering. *Mater. Sci. Eng. A* **2019**, *759*, 30–39. [CrossRef]
16. Li, Y.; Zeng, M.Q.; Liu, J.W.; Lu, Z.C. Evolution of metal nitriding and hydriding reactions during ammonia plasma-assisted ball milling. *Ceram. Int.* **2018**, *44*, 18329–18336. [CrossRef]
17. Aisyah, I.S.; Wyszomirska, M.; Calka, A.; Wexler, D. Nitrogenation of hafnium carbide powders in AC and DC plasma by Electrical Discharge Assisted Mechanical Milling. *J. Alloys Compd.* **2017**, *715*, 192–198. [CrossRef]
18. Nepapushev, A.A.; Buinevich, V.S.; Gallington, L.C.; Pauls, J.M.; Orlova, T.; Miloserdova, O.M.; Chapysheva, N.V.; Rogachev, A.S.; Mukasyan, A.S. Kinetics and mechanism of mechanochemical synthesis of hafnium nitride ceramics in a planetary ball mill. *Ceram. Int.* **2019**, *45*, 24818–24826. [CrossRef]
19. Chicardi, E.; Gotor, F.J.; Alcalá, M.D.; Córdoba, J.M. Effects of additives on the synthesis of TiC N by a solid-gas mechanically induced self-sustaining reaction. *Ceram. Int.* **2018**, *44*, 7605–7610. [CrossRef]
20. Córdoba, J.M.; Avilés, M.A.; Sayagués, M.J.; Alcalá, M.D.; Gotor, F.J. Synthesis of complex carbonitride powders $Ti_yM_{T1-y}C_xN_{1-x}$ (MT: Zr, V, Ta, Hf) via a mechanically induced self-sustaining reaction. *J. Alloys Compd.* **2009**, *482*, 349–355. [CrossRef]
21. Oghenevweta, J.E.; Wexler, D.; Calka, A. Early stages of phase formation before the ignition peak during mechanically induced self-propagating reactions (MSRs) of titanium and graphite. *Scr. Mater.* **2016**, *122*, 93–97. [CrossRef]
22. Córdoba, J.M.; Sayagués, M.J.; Alcalá, M.D.; Gotor, F.J. Monophasic $Ti_yNb_{1-y}C_xN_{1-x}$ nanopowders obtained at room temperature by MSR. *J. Mater. Chem.* **2006**, *17*, 650–653. [CrossRef]
23. Lutterotti, L.; Chateigner, D.; Ferrari, S.; Ricote, J. Texture, residual stress and structural analysis of thin films using a combined X-ray analysis. *Thin Solid. Films* **2004**, *450*, 34–41. [CrossRef]
24. Anstis, G.R.; Chantikul, P.; Lawn, B.R.; Marshall, D.B. A Critical Evaluation,of Indentation Techniques for Measuring Fracture Toughness: I, direct crack measurements. *J. Am. Ceram. Soc.* **1981**, *64*, 533–538. [CrossRef]
25. Merzhanov, A.G.; Rogachev, A.S. Structural Macrokinetics of SHS Processes. *Pure Appl. Chem.* **1992**, *64*, 941–953. [CrossRef]
26. Deevi, S.C. Structure of the Combustion Wave in the Combustion Synthesis of Titanium Carbides. *J. Mater. Sci.* **1991**, *26*, 2662–2670. [CrossRef]
27. Zhu, J.F.; Ye, L.; Tong, H.; Wang, F. Synthesis of Nanocrystalline $TiC_{1-X}N_x$ by High Energy Milling. In *Advanced Materials Research*; Trans Tech Publications Ltd.: Stafa-zuerich, Switzerland, 2011; Volume 194, pp. 458–461.

28. Chicardi, E.; Gotor, F.J.; Alcalá, M.D.; Córdoba, J.M. Influence of milling parameters on the solid-gas synthesis of TiC_xN_{1-x} by mechanically induced self-sustaining reaction. *Powder Technol.* **2017**, *319*, 12–18. [CrossRef]
29. Chicardi, E.; García-Garrido, C.; Beltran, A.M.; Sayagués, M.J.; Gotor, F.J. Synthesis of a cubic Ti(BCN) advanced ceramic by a solid-gas mechanochemical reaction. *Ceram. Int.* **2018**, *45*, 3878–3885. [CrossRef]
30. Chen, L.; Wang, Y.; Li, Y.; Zhang, X.; Meng, Q. Microstructural evolution, mechanical and thermal properties of TiC-ZrC-Cr_3C_2 composites. *Int. J. Refract. Met. Hard Mater.* **2019**, *80*, 188–194. [CrossRef]
31. Vorotilo, S.; Sidnov, K.; Sedegov, A.S.; Abedi, M.; Vorotilo, K.; Moskovskikh, D.O. Phase stability and mechanical properties of carbide solid solutions with 2–5 principal metals. *Comput. Mater. Sci.* **2021**, *201*, 110869. [CrossRef]
32. Buinevich, V.S.; Nepapushev, A.A.; Moskovskikh, D.O.; Trusov, G.V.; Kuskov, K.V.; Mukasyan, A.S. Mechanochemical synthesis and spark plasma sintering of hafnium carbonitride ceramics. *Adv. Powder Technol.* **2021**, *32*, 385–389. [CrossRef]
33. Buinevich, V.S.; Nepapushev, A.A.; Moskovskikh, D.O.; Kuskov, K.V.; Yudin, S.N.; Mukasyan, A.S. Ultra-high-temperature tantalum-hafnium carbonitride ceramics fabricated by combustion synthesis and spark plasma sintering. *Ceram. Int.* **2021**, *47*, 30043–30050. [CrossRef]
34. Jing, C.; Zhou, S.-J.; Zhang, W.; Ding, Z.-Y.; Liu, Z.-G.; Wang, Y.-J.; Ouyang, J.-H. Low temperature synthesis and densification of (Ti,V,Nb,Ta,Mo)(C,N) high-entropy carbonitride ceramics. *J. Alloys Compd.* **2022**, *927*, 167095. [CrossRef]
35. Zhang, M.; Wei, B.; Wang, D.; Fang, W.; Chen, L.; Wang, Y. Novel (Zr, Ti)(C, N)–SiC ceramics via reactive hot-pressing at low temperature. *Ceram. Int.* **2022**, *48*, 29641–29651. [CrossRef]
36. Yun, S.-S.; Han, B.-D.; Park, D.-S.; Kim, H.-D.; Lim, D.-S. Friction and wear of pressureless sintered Ti(C,N)–WC ceramics. *Wear* **2003**, *255*, 682–685. [CrossRef]